Available online at www.sciencedirect.com
SCIENCE DIRECT
Journal of Catalysis 235 (2005) 128–138
JOURNAL OF CATALYSIS
www.elsevier.com/locate/jcat

Alkylation of deactivated aromatic compounds on zeolites. Adsorption, deactivation and selectivity effects in the alkylation of bromobenzene and toluene with bifunctional alkylating agents

Sophie Van der Beken [a], Eileen Dejaegere [a], Kourosch A. Tehrani [b], Johan S. Paul [c], Pierre A. Jacobs [c], Gino V. Baron [a], Joeri F.M. Denayer [a,*]

[a] *Dienst Chemische Ingenieurstechniek, Vrije Universiteit Brussel, Pleinlaan 2, B-1050 Brussel, Belgium*
[b] *Dienst Organische Scheikunde, Vrije Universiteit Brussel, Pleinlaan 2, B-1050 Brussel, Belgium*
[c] *Centrum voor Oppervlaktechemie en Katalyse, Katholieke Universiteit Leuven, Kasteelpark Arenberg 23, B-3001 Leuven, Belgium*

Received 6 April 2005; revised 17 June 2005; accepted 24 June 2005

Available online 22 August 2005

Abstract

The alkylation of bromobenzene and toluene on zeolite H-USY (Si/Al 15) was studied using a high-throughput frontal analysis experimental setup. Adsorption properties of the involved components were determined using the batch technique. Reactions were performed using allyl alcohol, allyl acetate, 1-octen-3-ol, and allyl chloride as alkylating agents at 200 °C in the liquid phase. The reaction products could be divided into 3 fractions: (1) light components formed in side reactions of the alkylating agent; (2) primary alkylation products resulting from the alkylation of bromobenzene or toluene and subsequent rearrangement reactions; and (3) a heavy fraction consisting of secondary alkylation products and polyaromatics. Whereas the use of allyl chloride and 1-octen-3-ol as alkylating agents resulted mainly in the formation of undesired side products, bromobenzene was efficiently alkylated with allyl alcohol and allyl acetate, resulting in the formation of allyl bromobenzene, *cis*-2-propenyl bromobenzene, and *trans*-2-propenyl bromobenzene. The greatest product selectivity was obtained with allyl acetate, which is explained by the more favorable intrapore distribution of the alkylating agent and the aromatic substrate using allyl acetate as compared with allyl alcohol. Significant catalyst deactivation occurred in these reactions, attributed to pore blocking by very strong adsorption of side products in the zeolite micropores. With toluene, the product stream was dominated by heavy components, formed in secondary alkylation reactions.

Keywords: Zeolites; Alkylation; Bromobenzene; Allyl alcohol; Allyl acetate; Adsorption

1. Introduction

Friedel–Crafts alkylation reactions are important in the synthesis of intermediates in fine chemicals and pharmaceuticals [1–3]. Currently, most of these Friedel–Crafts alkylations are performed with corrosive Lewis acids such as $AlCl_3$ or BF_3. The inconveniences encountered with these homogeneous catalysts include difficult recovery of catalyst, corrosion of the working apparatus, and generation of toxic waste. Therefore, substitution of these homogeneous catalysts with cleaner heterogeneous catalysts, such as zeolites, is desirable. A particular type of challenging Friedel–Crafts reactions consists of alkylation reactions of deactivated haloaromatics with bifunctional molecules. Here the alkylating agent used contains two functionalities, the first to allow substitution on the aromatic ring and the second to allow further functionalization in subsequent reaction steps. The halogen atom acts as a protecting group for the aromatic ring during further functionalization of the previously added alkyl group. Highly acid catalysts are required to promote such alkylation and acylation reactions because of the deactivated

* Corresponding author. Fax: +32-2-6293248.
E-mail address: joeri.denayer@vub.ac.be (J.F.M. Denayer).

0021-9517/$ – see front matter
doi:10.1016/j.jcat.2005.06.029

character of the aromatic ring as a result of the electron-withdrawal effect of the halogen substituent.

Zeolites have already proven their viability in acylation reactions and alkylation reactions [4–17]. Hu [18] compared the benzylation of deactivated and activated aromatics using a series of zeolites. The shape selectivity of the zeolites was much less pronounced using more reactive aromatics like toluene or ethylbenzene, indicating that the reaction with these substrates proceeded at the surface of the porous catalysts. Using deactivated aromatic substrates, such as halobenzenes, the reaction proceeded in the catalyst pores, resulting in better control of the product selectivity. Beers [14] reported on the acylation of anisole with octanoic acid using zeolite H-BEA. The catalytic activity appeared to depend on the mesoporosity and the Si/Al ratio of the zeolite. Derouane [10,11] studied adsorption, reaction, and deactivation of zeolite H-BEA in the acetylation of anisole with acetic acid as the acylating agent. Deactivation of the catalyst occurred due to both product inhibition by *p*-methoxyacetophenone and dealumination by acetic acid formed during the reaction. These authors concluded that competitive adsorption effects could play a major role when applying zeolites to fine chemical synthesis. In certain cases, very strong adsorption of the reaction products on the active sites can even lead to catalyst deactivation [11,19,20]. Such competitive adsorption effects can be expected in Friedel–Crafts-type alkylation reactions with zeolites, because molecules of completely different physiochemical nature are involved (i.e., aromatic substrate and alkylating agents such as alcohols, esters, anhydrides, etc.).

In the present work, adsorption, kinetic, and deactivation aspects in alkylation reactions of deactivated aromatic compounds with bifunctional alkylating agents on zeolites are studied. In particular, the alkylation of bromobenzene and toluene with allyl alcohol, allyl acetate, 1-octen-3-ol, and allyl chloride on zeolite H-USY is studied. A high-throughput device for measuring adsorption, deactivation, and catalytic activity in the liquid phase was constructed for this purpose. The relationship between observed catalytic selectivity and adsorption properties is discussed. In the second of this series of research papers, the effect of operating conditions and zeolite type/composition on the reaction patterns is studied in closer detail. Finally, in the third paper kinetic models are developed and tested for significance. Optimization of the reaction conditions to obtain maximal product yield is performed.

2. Experimental

2.1. Analytical techniques

The components in the reaction mixture were identified by gas chromatography time-of-flight mass spectrometry (GC-MS) (LECO Pegasus III). The GC unit was equipped with an HP-5 ((5%-diphenyl)-dimethylsiloxane) capillary column with a length of 30 m, internal diameter of 320 µm, and film thickness of 0.25 µm. Most of the components could be directly identified, but for some of the alkylation products, several structural isomers were obtained that could not be discriminated by GC-MS. Several of these alkylation products (i.e., *p*-allyl bromobenzene, *cis*- and *trans*-*p*-propenyl bromobenzene, and *cis*- and *trans*-*o*-propenyl bromobenzene) were prepared by organic synthesis, and identified using ^{1}H nuclear magnetic resonance (NMR), which allowed assignment of the peaks in the chromatogram. After peak identification, classical GC analysis was performed, using the same column and method as used in the GC-MS analysis. Polymers present in the reactor effluent were analyzed by Fourier transform infrared (FTIR) and Raman IR analyses of a thin polymer film obtained after evaporation of the reaction mixture on a glass plate. Micropore volume and surface area of selected catalysts were determined using N_2-porosimetry and applying the BET method.

2.2. Components

The alkylating agents allyl alcohol, allyl acetate, 1-octen-3-ol, and allyl chloride, each with a minimum purity of 98%, were obtained from Fluka. The substrates toluene and bromobenzene (Fluka) had a purity of 99.5%.

2.3. Catalysts

The H-USY zeolite CBV720 (Si/Al 15) (Zeolyst International) was activated by heating to 400 °C at a rate of 2 °C/min under constant nitrogen flow. Pore volume and acidic properties of this catalyst were determined in earlier work and are specified in Table 1 [21,22].

2.4. Catalytic experiments

A high-throughput frontal analysis setup was constructed to perform continuous-flow catalytic and adsorption experiments (Scheme 1). Eight parallel channels each consisting of a high-pressure liquid pump, a pneumatic-driven waste valve, and a stainless steel catalytic column, were attached to a in-house-developed pneumatic-driven automated fraction collector, enabling sample collection of each channel

Table 1
Catalyst properties

	CBV720
Bulk Si/Al ratio	13
Micropore volume[a] (cc/g)	0.27
Mesopore volume[a] (cc/g)	0.15
Acid site concentration[b] (mmol/g)	0.62
Weak	0.06
Strong	0.54

[a] Determined with nitrogen porosimetry at 77 K [21].
[b] Determined with ammonia TPD (data from Refs. [21,22]): weak sites, $\Delta H = 90$–95 kJ/mol; strong sites, $\Delta H = 115$–127 kJ/mol.

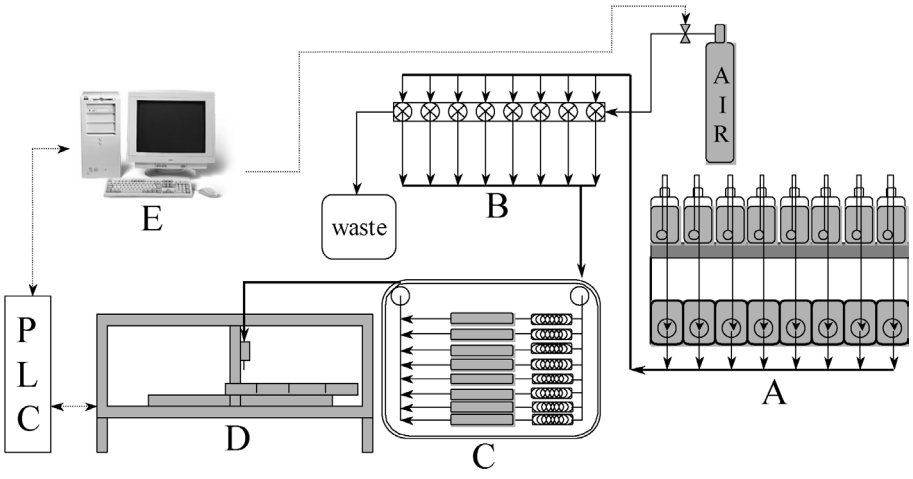

Scheme 1. Flow-chart of the high-throughput frontal analysis set-up for continuous flow catalytic experiments: (A) 8 high-pressure liquid pumps; (B) pneumatic driven three-way valves directing the liquid flow to a waste container in one position and to the catalytic columns in the other position; (C) ventilated oven containing 8 catalytic columns, the feed is preheated by passing through a loop of 1.3 m capillary tubing; (D) home-designed fully automated septum piercing fraction collector controlled via PLC; (E) computer used to program the PLC and to control the pneumatic driven valves.

separately in closed vials at any chosen time during the reaction experiment. The sampling system allows collection of 800 liquid reactor effluent samples in a single run. Septum piercing probes inject 500 µl of the reactor effluent into a 2-ml vial with insertion through the septum used to close the vial. The racks, containing 100 sample vials, can be directly transferred to the CTC PAL autoinjector mounted on the GC unit, allowing efficient analysis of the samples.

The connections between the different parts of the setup were all made with 2-mm i.d. stainless steel tubing. The columns (5 cm long and 4.5 mm i.d.) were packed with about 0.4 g of catalyst particles. Before the reaction mixture entered the catalytic column, it was preheated by passing it through 1.3-m loop placed in the oven together with the catalytic column. A backpressure at the outlet of the catalytic column was generated with 2.5-mm loop of capillary tubing, guaranteeing liquid phase conditions in the catalytic column for all experiments.

As a strongly deactivated aromatic component, bromobenzene was chosen and was compared with the activated aromatic component toluene. As alkylating agents, allyl alcohol, allyl acetate, allyl chloride, and 1-octen-3-ol were tested. The alkylating agent/substrate mixture was pumped through the catalytic column at a feed flow rate of 0.2 ml/min (liquid hourly space velocity = 57.6 h^{-1}). The experiments were performed at 200 °C. The reactor feed consisted of a mixture of 1/40 molar ratio of the alkylating agent/substrate.

2.5. Batch adsorption experiments

Adsorption isotherms of the components tested in the catalytic experiments were determined using the batch technique on a series of faujasites at room temperature. The details of the method have been described elsewhere [23]. The following Y and USY zeolites (Zeolyst International) were tested: CBV500 (Si/Al 2.7), CBV712 (Si/Al 6), CBV720 (Si/Al 15), CBV760 (Si/Al 30), and CBV780 (Si/Al 40). CBV500 and CBV712 were provided as ammonium-exchanged zeolites and transformed into their protonic form by heating to 550 °C in a muffle oven, at a heating rate of 2 °C/min. The zeolites were activated by heating to 400 °C at a rate of 2 °C/min under a constant nitrogen flow. The experimental isotherms were fitted to the Langmuir equation (1) to obtain the adsorption constant (K') and the adsorption capacity (q_s) of the studied components,

$$\frac{q}{q_s} = \frac{bC}{1+bC} \quad \text{or} \quad q = \frac{K'C}{1+bC}, \tag{1}$$

with

$$K' = bq_s. \tag{2}$$

3. Results and discussion

Binary adsorption isotherms of different alkylating agents in bromobenzene were determined to obtain a first idea of competitive adsorption effects that could occur in the studied alkylation reaction. In a next step, the same components were catalytically tested using zeolite H-USY (Si/Al 15).

3.1. Adsorption

Fig. 1 shows adsorption isotherms of allyl alcohol, allyl acetate, allyl chloride, and 1-octen-3-ol in bromobenzene as bulk solvent on zeolite H-Y (Si/Al ratio 2.7) at room temperature. The corresponding adsorption constants are given in Table 2. All of these components except allyl chloride are very selectively adsorbed. Already at very low bulk liquid concentrations (0.0001–0.001 g/g), half of the zeolite pore volume is filled with these components. Allyl chloride shows no adsorption selectivity on zeolite H-Y, indicating that the

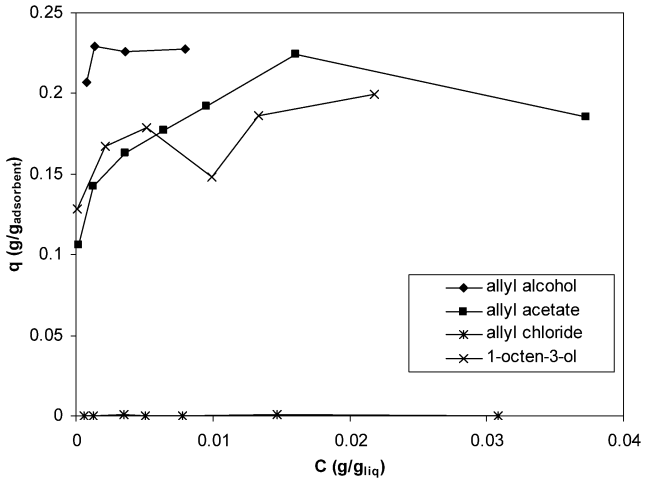

Fig. 1. Adsorption isotherms of allyl alcohol, allyl acetate, allyl chloride and 1-octen-3-ol in bromobenzene on H-Y (Si/Al 2.7) at room temperature.

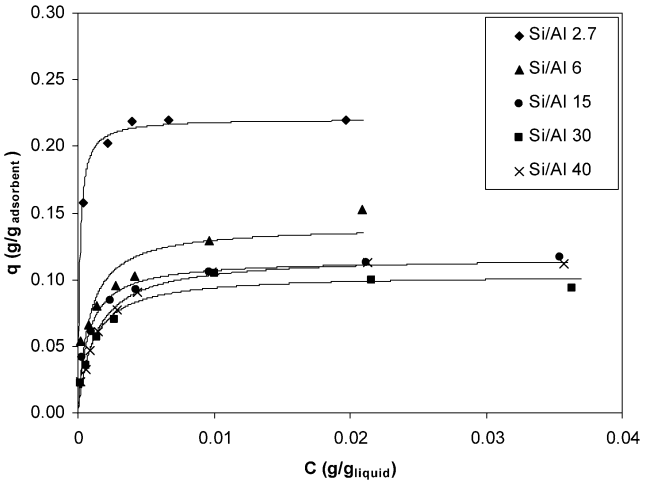

Fig. 2. Adsorption isotherms (markers) and Langmuir fit curves (lines) of allyl alcohol in bromobenzene on H-Y (Si/Al 2.7) and H-USY zeolites with different Si/Al ratio at room temperature.

Table 2
Adsorption constant (K') and adsorption capacity (q_s) of allyl alcohol, 1-octen-3-ol, allyl acetate and allyl chloride on zeolite H-Y (Si/Al 2.7) with bromobenzene as solvent (room temperature)

Adsorbate	K' ($g/g_{adsorbent}$)/(g/g_{liquid})	q_s ($g/g_{zeolite}$)	q_s (molecules/supercage)
Allyl alcohol	3120	0.23	5.6
1-Octen-3-ol	2480	0.18	2.0
Allyl acetate	960	0.18	3.2
Allyl chloride	<1	$<10^{-3}$	$<10^{-3}$

Table 3
Langmuir parameters of allyl alcohol on a series of H-Y and H-USY zeolites with different Si/Al ratio at room temperature

Si/Al	K' ($g/g_{adsorbent}$)/(g/g_{liquid})	q_s ($g/g_{adsorbent}$)
2.5	3120	0.23
6	170	0.14
15	150	0.11
30	100	0.10
40	90	0.12

presence of a halogen functionality or a double bond does not result in a more specific interaction with the zeolite compared with bromobenzene. With allyl alcohol, a plateau in the adsorption isotherm is reached at a fractional volumetric pore filling of about 90%, corresponding to 5.6 molecules of allyl alcohol adsorbed per supercage (see Table 2). With allyl acetate, diallyl ether, and 1-octen-3-ol, each of which has a molecular size practically twice that of allyl alcohol, between 70 and 80% of the available pore volume is used, corresponding to 3.2, 2.6, and 2 molecules/supercage, respectively. Allyl alcohol shows the highest adsorption selectivity as a result of the very strong interaction of the hydroxyl group with the Brønsted acid site of the zeolite (Table 2).

Adsorption isotherms of allyl alcohol on a H-Y zeolite (Si/Al 2.7) and a series of H-USY zeolites with different Si/Al ratio (6, 15, 30, and 40) in bromobenzene are shown in Fig. 2. Allyl alcohol is very selectively adsorbed on zeolite H-Y. This zeolite is not dealuminated and has the highest polarity of the studied materials. With increasing degree of dealumination, the selectivity and capacity for allyl alcohol decreases. Beyond a Si/Al ratio of 15, the adsorption capacity remains nearly constant. From this Si/Al ratio, most of the aluminum atoms are isolated, and further dealumination of the zeolite no longer affects adsorption (Table 3) [24].

3.2. Catalytic tests

Zeolite H-USY, with a Si/Al ratio of 15, was used. The adsorption selectivity for the alkylating agents over the aromatic substrate of this zeolite is pronounced, but much lower than that for the faujasites with lower Si/Al ratios (Fig. 2). In contrast, the adsorption capacity is nearly unaffected by further dealumination beyond a Si/Al of 15, whereas the number of acid sites decreases proportionally to the aluminum content. Hence this zeolite can be expected to show a good compromise between adsorption selectivity and catalytic activity.

The conversion of the different alkylating agents in the alkylation of bromobenzene is shown in Fig. 3 as a function of time on stream (TOS). Complete conversion of the alkylating agent is observed in an initial period, but pronounced deactivation of the catalyst occurs. After 70–150 min, the conversion of allyl alcohol and allyl acetate starts to decrease, whereas the conversion of allyl chloride and 1-octen-3-ol remains close to 100% constant during the entire run. After 400 min on stream, the conversions of allyl acetate and allyl alcohol drop to 0 and 40%, respectively.

Analysis of the reactor effluent by GC-MS showed formation of a broad family of components. In general, (1) light- to intermediate-weight components, such as propene, propanal, and propanol, formed in side reactions of the alkylating

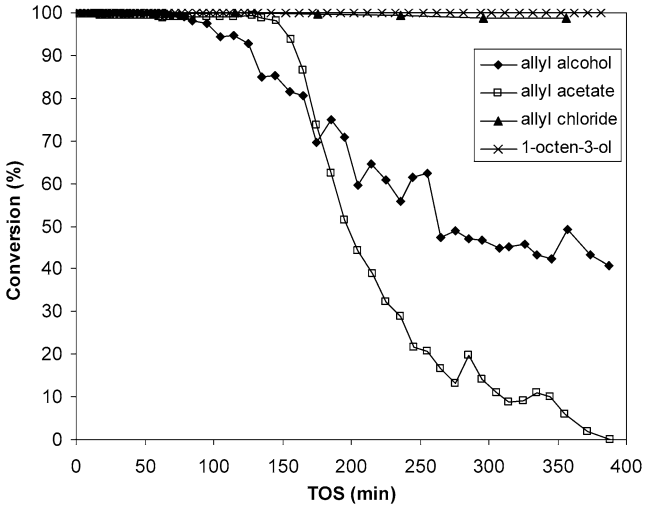

Fig. 3. Conversion of allyl alcohol, allyl acetate, allyl chloride and 1-octen-3-ol in the alkylation of bromobenzene at 200 °C as a function of time on stream (TOS) (liquid hourly space velocity, LHSV = 57.6 h^{-1}).

agent itself; (2) components with an intermediate molecular weight, such as allyl bromobenzene and propenyl bromobenzene, formed in the alkylation of the aromatic substrate; and (3) heavy components formed in oligomerization reactions or secondary alkylation reactions, such as 1-bromo-2-(2-methyl-pent-4-enyl)-benzene and 1-bromo-2-(1-ethyl-but-3-enyl)-benzene, were observed. Fig. 4 shows the product distribution during the entire run for the four alkylating agents. A more detailed overview of the main reaction products is given in Table 4, together with the total amount produced in 6 h TOS.

The total turnover number (TON), defined as the number of allyl acetate molecules converted per acid site, and the alkylation TON, defined as the number of mono-alkylated products produced per acid site, are given in Table 3. With allyl acetate, the lowest total TON is found (49.9 catalytic cycles/acid site), as is, in contrast, the highest number of alkylation product molecules formed per acid site (27.9). The other alkylating agents show low alkylation TONs (<7 alkylation reactions per acid site), but rather high total TONs, indicating that the reaction occurs in a less selective way with allyl alcohol, allyl chloride, and 1-octen-3-ol.

With allyl alcohol, the light fraction consisted of propene, propanal, propanol, and diallyl ether, the latter being the condensation product of allyl alcohol (Table 4). The amount of light products increases steeply from almost zero at the start of the catalytic run to a maximum after 200 min TOS, and then decreases slightly (Fig. 4a) (vide supra). Chemisorption of allyl alcohol on the Brønsted acid site of the zeolite, followed by protonation, results in formation of water and an

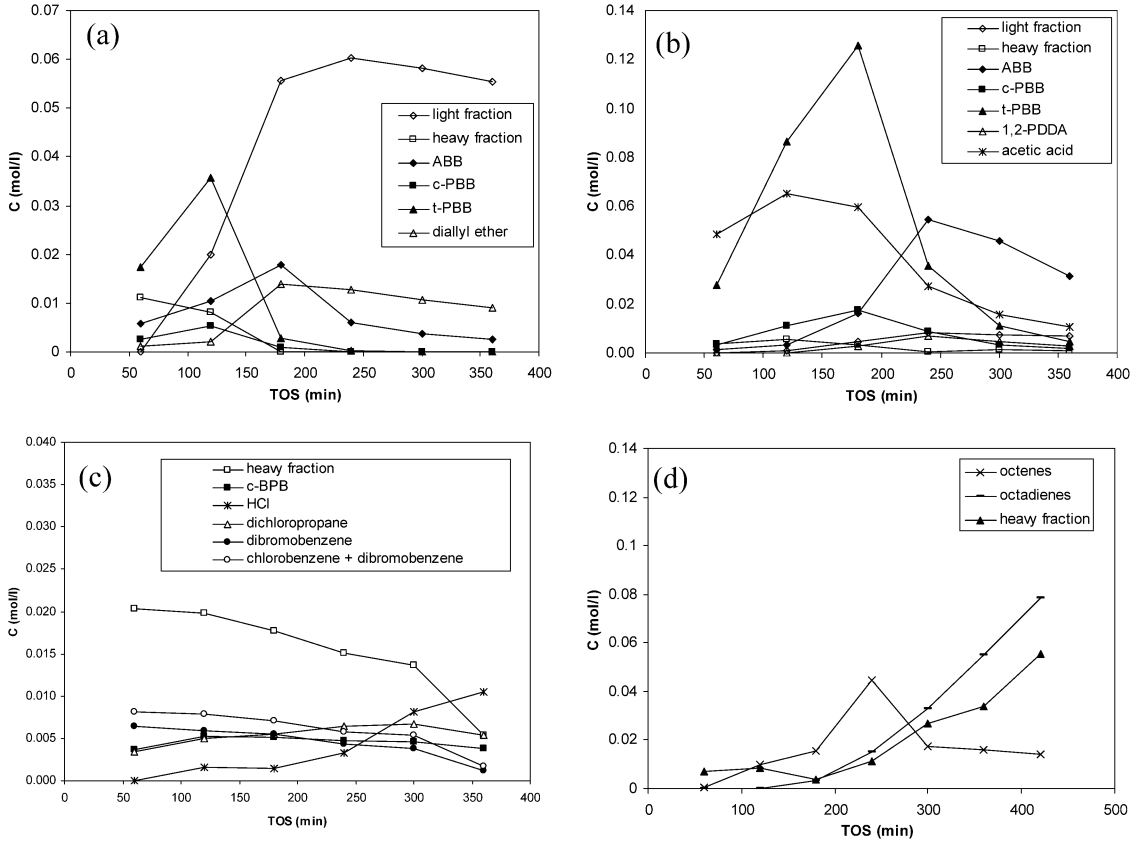

Fig. 4. Composition of the reactor effluent in the alkylation of bromobenzene with (a) allyl chloride, (b) 1-octen-3-ol, (c) allyl alcohol and (d) allyl acetate on zeolite H-USY (Si/Al 15) at 200 °C (ABB, allyl bromobenzene; c-PBB, *cis*-propenyl bromobenzene; *t*-PBB, *trans*-propenyl bromobenzene; 1,2-PDDA, 1,2-propanediol diacetate).

Table 4
Products formed (expressed in moles) during 6 h of reaction with allyl alcohol, allyl acetate, allyl chloride and 1-octen-3-ol as alkylating agent and bromobenzene as substrate on H-USY (Si/Al 15) at 200 °C (LHSV = 57.6 h^{-1})

	Product	Formula	Product formed in 6 h TOS (mol)			
			Allyl alcohol	Allyl acetate	Allyl chloride	1-octen-3-ol
Side products of alkylating agent	Propene	C_3H_6	2.21×10^{-4}	6.16×10^{-5}	–	–
	Propanal	C_3H_6O	1.00×10^{-3}	1.45×10^{-4}	–	–
	Propanol	C_3H_8O	1.77×10^{-3}	–	–	–
	Ethyl acetate	$C_4H_8O_2$	–	7.43×10^{-5}	–	–
	Propyl acetate	$C_5H_{10}O_2$	–	5.82×10^{-5}	–	–
	Acetic acid	$C_2H_4O_2$	–	2.73×10^{-3}	–	–
	Hydrogen chloride	HCl	–	–	2.98×10^{-4}	–
	Diallyl ether	$C_6H_{10}O$	5.96×10^{-4}	–	–	–
	1,2-PDDA	$C_7H_{12}O_4$	–	2.08×10^{-4}	–	–
	Dichloropropane	$C_3H_6C_{l2}$	–	–	3.87×10^{-4}	–
	Octene isomers	C_8H_{16}	–	–	–	1.24×10^{-3}
	Octadienes	C_8H_{14}	–	–	–	1.28×10^{-3}
	Sum (side products of AA)		$\mathbf{3.59 \times 10^{-3}}$	$\mathbf{3.28 \times 10^{-3}}$	$\mathbf{6.85 \times 10^{-4}}$	$\mathbf{2.52 \times 10^{-3}}$
Intermediate fraction: desired alkylation products	Allyl bromobenzene	C_9H_9Br	5.56×10^{-4}	1.83×10^{-3}	2.47×10^{-4}	0
	cis-2-Propenyl bromobenzene	C_9H_9Br	1.07×10^{-4}	5.46×10^{-4}	3.27×10^{-4}	0
	trans-2-Propenyl bromobenzene	C_9H_9Br	6.74×10^{-4}	3.49×10^{-3}	0	0
	Sum (intermediate fraction)		$\mathbf{1.34 \times 10^{-3}}$	$\mathbf{5.86 \times 10^{-3}}$	$\mathbf{5.74 \times 10^{-4}}$	**0**
Heavy fraction	**Sum (heavy fraction)**		$\mathbf{2.29 \times 10^{-4}}$	$\mathbf{1.89 \times 10^{-4}}$	$\mathbf{1.10 \times 10^{-3}}$	$\mathbf{1.08 \times 10^{-3}}$
Total turn over number (molecules/acid site)			**63.8**	**49.3**	**82.4**	**96.0**
Alkylation turn over number (molecules/acid site)			**6.4**	**27.9**	**2.7**	**0**

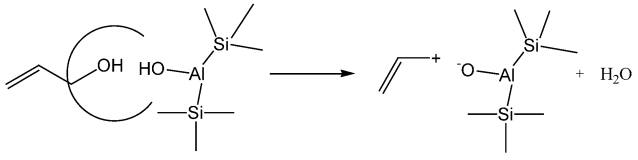

Scheme 2. Formation of the allylic carbocation and water resulting from the chemisorption of allyl alcohol on the zeolite Brønsted site.

allylic species on the acid site [25]; see Scheme 2. (We note here that water was not quantified in our analysis.) Diallyl ether is most likely formed in the reaction between allyl alcohol and the allylic cation (Scheme 3). Propanal, propanol, and propene are possibly formed through decomposition of diallyl ether or by direct rearrangement, hydrogenation, or dehydration of allyl alcohol.

Electrophilic aromatic substitution of a proton from the aromatic ring with the allylic carbocation gives the desired alkylation product allyl bromobenzene (Scheme 4). Successive protonation of the double bond and elimination of a proton in allyl bromobenzene gives rise to a mixture of *trans*- and *cis*-2-propenyl bromobenzene (Scheme 5). *cis*-2-Propenyl bromobenzene, the least stable isomer, is formed in the lowest concentration (Table 4 and Fig. 4a). At the beginning of the run, *trans*-2-propenyl bromobenzene is the most abundant alkylation product, followed by allyl bromobenzene and *cis*-2-propenyl bromobenzene. In the initial 130 min, an increase in the *trans*- and *cis*-2-propenyl bromobenzene concentration is observed. This can be explained by a partial conversion of *trans*- and *cis*-2-propenyl bromobenzene into very heavy products, remaining on the

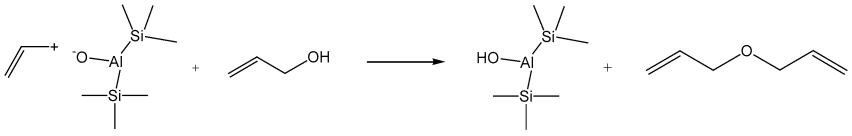

Scheme 3. Reaction between a protonated allyl alcohol and the allylic carbocation leading to the formation of diallyl ether.

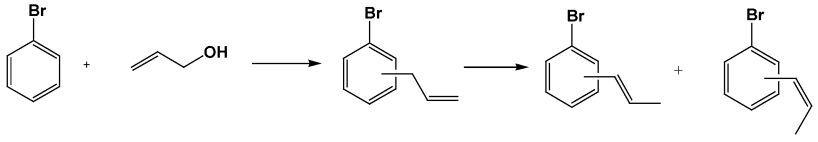

Scheme 4. Alkylation products in the alkylation of bromobenzene with allyl alcohol.

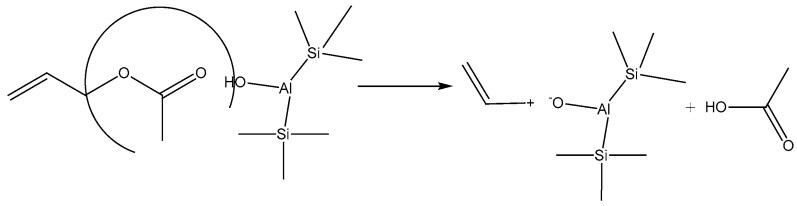

Scheme 5. Formation of the allylic carbocation and acetic acid resulting from the chemisorption of allyl acetate on the zeolite Brønsted site.

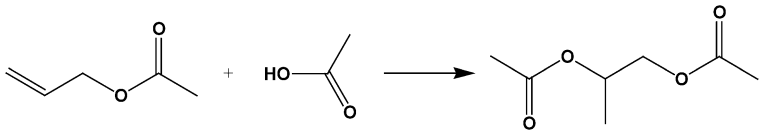

Scheme 6. Formation of 1,2-propandiol diacetate in the reaction between allyl acetate and its leaving group acetic acid.

catalyst surface, at the beginning of the run as a result of the very high initial activity of the catalyst (Fig. 3). These heavy products block the active sites and reduce the overall catalyst activity such that less *trans*- and *cis*-2-propenyl bromobenzene is converted into heavy components after this initial period, leading to a higher *trans*- and *cis*-2-propenyl bromobenzene yield. After 130 min TOS, the *trans*- and *cis*-2-propenyl bromobenzene concentration starts to decrease, while at the same time the allyl bromobenzene fraction increases. Because of catalyst deactivation, less of the primary alkylation product allyl bromobenzene is converted into *cis*- and *trans*-2-propenyl bromobenzene. Finally, a group of heavier components, resulting from a second alkylation of the aforementioned products and polymerization reactions of allyl alcohol, was observed. The amount of heavy products decreases with TOS to reach zero after about 200 min. Because most of these unwanted side reactions are (Brønsted) acid-catalyzed, less secondary alkylation and polymerization occurs with higher catalyst deactivation.

With allyl acetate, the "light" fraction consisted of propene, propanal, ethyl acetate, propyl acetate, and acetic acid (Table 4). The mechanisms of propene and propanal formation are similar to those of allyl alcohol formation. Acetic acid, the most abundant light product (63% of the light fraction), is formed in the decomposition of allyl acetate on the Brønsted acid site (Scheme 5). A somewhat heavier component, 1,2-propandiol diacetate, was formed in nonnegligible amounts (Table 4). 1,2-propandiol diacetate is formed in the reaction between allyl acetate and its leaving group acetic acid (Scheme 6).

The alkylation products (allyl bromobenzene, *cis*-2-propenyl bromobenzene, and *trans*-2-propenyl bromobenzene) are the same as those found with allyl alcohol as the alkylating agent (see Table 4). The evolution of these components with TOS is similar to that observed with allyl alcohol (Fig. 4b): initially, *trans*-2-propenyl bromobenzene is the dominant alkylation product, demonstrating an increasing concentration during the first 180 min followed by a decreasing concentration with an increasing allyl bromobenzene concentration. From 250 min TOS onward, allyl bromobenzene becomes the dominant alkylation product. *cis*-2-Propenyl bromobenzene follows the same profile as *trans*-2-propenyl bromobenzene but is produced in much lower concentrations. For each of these components, the *ortho*-, *meta*-, and *pararegio*- isomers were found. The average distribution of the structural isomers depended slightly on the alkylation product, but in general the *ortho*-isomer is the most dominant isomer followed by the *para*-isomer, whereas only small amounts of the *meta*-isomer are formed (see Table 3). This corresponds to the *ortho*/*para*-directing nature of bromobenzene. The absolute amount of the primary alkylation products is significantly higher here than in the reaction with allyl alcohol (Table 4). With allyl acetate, a heavier product, formed via a secondary alkylation of allyl bromobenzene, *cis*-2-propenyl bromobenzene, or *trans*-2-propenyl bromobenzene, is also formed. The heavy fraction decreases with TOS, whereas the light fraction has the opposite tendency.

The alkylation reactions performed with allyl chloride and 1-octen-3-ol resulted in the formation of a great amount of side products of alkylating agent and heavy components and only a low amount of primary alkylation products despite the high conversion level during the entire run (see Table 2). In the reaction with allyl chloride, the main product fraction consisted of heavy products. Not all of these heavy products could be quantified correctly, because of their long retention times in the GC analysis. Traces of bromocumene, propyl bromobenzene, chlorobenzene, and dibromobenzene were detected. Formation of an allylic cation starting from allyl chloride requires Lewis acid catalysis. Although faujasites are known to contain Lewis acidity [26], the number of Lewis acid sites is much smaller than the number of Brønsted acid sites. Moreover, allyl chloride is only weakly adsorbed from its mixture with bromobenzene by the zeolite catalyst (see Fig. 1). Because of the aforementioned lack of sufficient Lewis acidity in these zeolites, other degradation/reaction mechanisms are responsible for the formation of the side products. Hence formation of the allylic cation will occur with a much lower efficiency here than in allyl alcohol and allyl acetate, explaining the low amounts of allyl bromobenzene and *cis*- and *trans*-2-propenyl bromobenzene formed. Compared with allyl alcohol, where the

oxygen atom is far more basic than the double bond, allyl chloride is almost completely protonated at the double bond. In general, HCl is formed in all kinds of side reactions as a result of elimination reactions (Fig. 4c). The large amount of heavy products can be explained by a catalytic act of HCl. HCl present in the product stream in the reactor bed catalyzes polymerization and alkylation reactions through protonation of the double bond of allyl chloride, explaining the complete conversion of allyl chloride. Part of HCl is consumed in exchange reactions with Br on the aromatic ring, producing chlorobenzene and dibromobenzene (Fig. 4c). Adding HCl to allyl chloride leads to the formation of dichloropropane. With increasing TOS, the amount of HCl increases, indicating that less HCl is consumed in such reactions. Observed heavy product formation decreases with TOS, although the allyl chloride conversion is >95% during the entire run. It thus appears that a large fraction of very heavy products builds up in the catalyst bed, either in the catalyst pores or on its external surface. A detailed study of this coking mechanism is beyond the scope of this work.

With 1-octen-3-ol, a large amount of heavy products was also formed, along with a range of octadienes and octene isomers in high concentrations (Fig. 4d and Table 4). The concentration of these components in the reactor effluent increases with increasing TOS. No alkylation products were detected. Compared with allyl alcohol, 1-octen-3-ol has the potential to eliminate water, thus leading to 1,3-octadiene. Further oligomerization and cracking reactions result in octene formation. Furthermore, octene and octadiene may polymerize into high molecular weight components. At the beginning of the run, when the catalyst has the highest activity, very heavy polymers are formed that remain trapped in the catalyst pores. With increasing TOS, parts of the micropores become saturated with heavy components and the activity gradually decreases, so the polymerization reactions stop at an earlier stage and increasing amounts of octene and octadiene are detected. During the time frame of the experiment, sufficient catalytic activity remains for complete conversion of 1-octen-3-ol through this dehydrogenation mechanism. Despite this, however, formation of an allylic cation by protonation followed by substitution on the aromatic ring does not seem to occur in the present test conditions, possibly because water is eliminated much more rapidly from 1-octen-3-ol (i.e., formation of a conjugated double bond).

In summary, it appears that allyl chloride and 1-octen-3-ol are less suitable alkylating agents than allyl alcohol and allyl acetate. Thus the remainder of this paper focuses on the effects observed with the latter two components. The total amount of light side products (from propene to propyl acetate; Table 4) formed in 6 h of run using allyl alcohol as the alkylating agent was approximately one order of magnitude higher (2.99×10^{-3} mol) than the alkylation with allyl acetate (3.39×10^{-4} mol). Allyl acetate leads to about four-fold greater production of primary alkylation products (allyl bromobenzene, *cis*-2-propenyl bromobenzene, and *trans*-2-propenyl bromobenzene) (Table 4). Finally, the conversion of allyl acetate decreases more rapidly with time than does that of allyl alcohol (Fig. 3). However, with allyl alcohol, mainly light breakdown components and diallyl ether are formed from approximately 120 min TOS onward, whereas with allyl acetate, significantly less light products are formed.

One factor responsible for this difference in alkylation efficiency between allyl alcohol and allyl acetate might be found in adsorption effects. The adsorption selectivity for allyl alcohol on zeolite H-USY is higher than that for allyl acetate because of the presence of the hydroxyl group in allyl alcohol. Using the same concentration of the alkylating agents in both reactions will result in a significantly higher concentration of allyl alcohol than allyl acetate in the zeolite pores. On the one hand, this will promote side reactions of allyl alcohol, which is translated in the high reaction selectivity for the lighter fraction (Fig. 4a), and formation of polymers, as discussed earlier. On the other hand, the amount of bromobenzene in the zeolite pores will be lower with allyl alcohol as the alkylating agent, resulting in lower efficiency for the bimolecular alkylation between bromobenzene and allyl alcohol. The allyl acetate/bromobenzene ratio in the zeolite pores is more favorable for the alkylation reaction because of the lower adsorption selectivity for allyl acetate.

Deactivation of the zeolite should be explained by a formation of heavy and/or strongly adsorbing components (polymers) inside the zeolite pores, which first block the active sites and gradually fill up the entire pore volume. A *t*-plot analysis of the nitrogen adsorption isotherms of a fresh zeolite sample and a sample obtained after the catalytic run indeed showed a loss of micropore volume from 0.27 to 0.11 cc/g. Presence of polymers was demonstrated by FTIR and Raman-IR spectroscopy of the reaction product obtained in batch reaction experiments. Polymer formation or irreversible adsorption of side products in the pores reduces the pore space such that steric constraints impede the bimolecular reaction between bromobenzene and allyl alcohol, resulting in a decrease in activity with time. Side reactions of allyl alcohol, leading to formation of light components (i.e., propene, propanal, and propanol), can still occur in this reduced pore volume.

Also with allyl acetate, formation of heavy and/or strongly adsorbing components inside the zeolite pores results in an even faster decrease in catalytic activity compared with allyl alcohol (Fig. 1). Again, the reduced pore volume results in decreased efficiency of the bimolecular reaction between bromobenzene and allyl acetate. But allyl acetate itself is much less sensitive than allyl alcohol to transformation into light products in this reduced pore volume. Again this may be explained by the lower adsorption selectivity of allyl acetate, resulting in a decreased likelihood of condensation reactions and subsequent decomposition reactions into light products. An argument in favor of this hypothesis stems from the absence of dimerization products of allyl acetate. Fur-

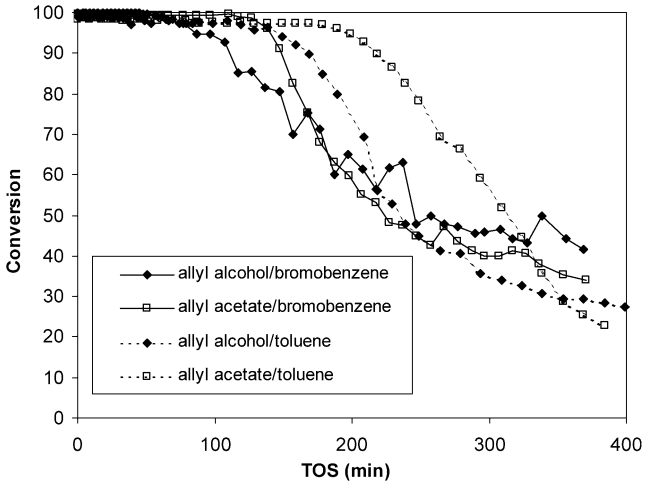

Fig. 5. Conversion of allyl alcohol and of allyl acetate in the alkylation of bromobenzene (full line) and toluene (dashed line) on zeolite H-USY (Si/Al 15) at 200 °C as a function of TOS (LHSV = 57.6 h^{-1}).

thermore, batch adsorption experiments have indicated that in a fresh Y-zeolite, almost six allyl alcohol molecules can be adsorbed per supercage, compared with only three allyl acetate molecules per supercage (Table 2). This observation also provides evidence in favor of the aforementioned mechanism.

However, an alternative explanation is that acetic acid, formed in the decomposition of allyl acetate (see Scheme 5), results in irreversible destruction of the zeolite acidity through dealumination, explaining the total loss of activity [10]. To verify this hypothesis, a deactivated catalyst was calcined at 500 °C and reused in a catalytic test. The reactivated catalyst was as active as the fresh catalyst in the alkylation of bromobenzene with allyl acetate, indicating that the zeolite activity is not affected by acetic acid.

3.3. Deactivated versus activated aromatic rings

Two additional experiments with allyl alcohol and allyl acetate were performed using toluene as the substrate, under similar operating conditions as those applied with bromobenzene. Fig. 5 compares the conversion of allyl acetate and allyl alcohol for both substrates. For allyl alcohol, the difference in deactivation rate was relatively small, but with allyl acetate, the conversion decreased much less rapidly with toluene than with bromobenzene. The product distribution also differed pronouncedly between the two substrates (Figs. 4 and 6). The detailed product distribution is given in Table 4.

In the alkylation of toluene with allyl acetate, the light fraction consisted of propene and propanal, while nearly no ethyl acetate, propyl acetate, or 1,2-propandiol diacetate were observed. With toluene as the substrate, about threefold less light reaction products (propene to propyl acetate) were formed compared with bromobenzene (Tables 4 and 6). The amount of primary alkylation products (allyl toluene) was almost eightfold lower with toluene, despite higher global

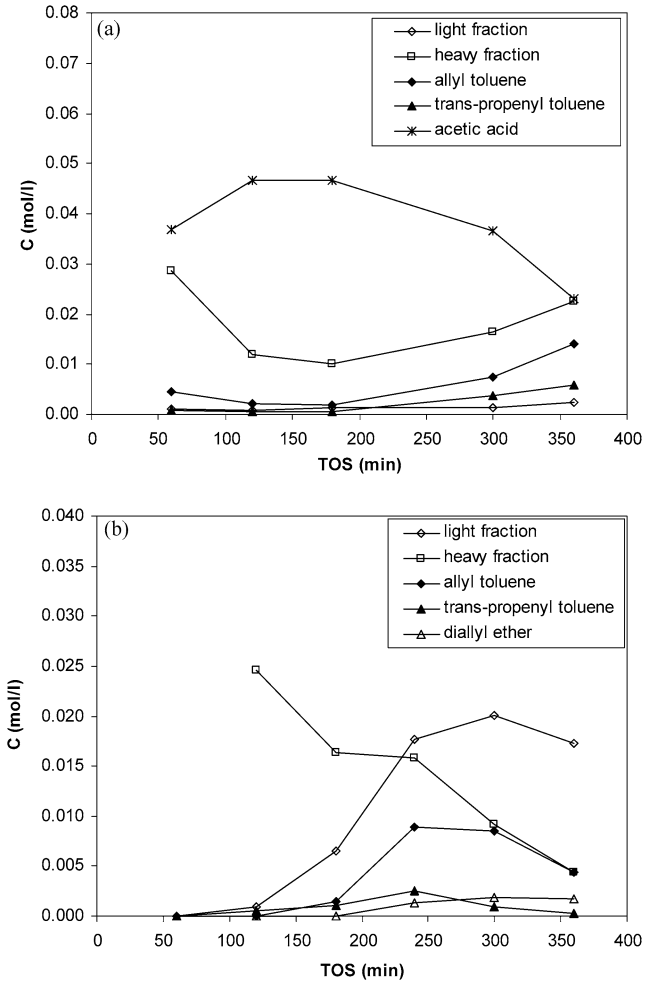

Fig. 6. Product distribution in the alkylation of toluene with (a) allyl alcohol and (b) allyl acetate on H-USY (Si/Al 15) (200 °C, LHSV = 57.6 h^{-1}).

Table 5
Distribution of the structural isomers of the alkylation products allyl bromobenzene, *cis*-2-propenyl bromobenzene and *trans*-2-propenyl bromobenzene formed in the alkylation of bromobenzene with allyl alcohol and with allyl acetate on H-USY (Si/Al 15) at 200 °C

	Product formed in 6 h (mol)		Product distribution (%)	
	Allyl alcohol	Allyl acetate	Allyl alcohol	Allyl acetate
o-ABB	3.60×10^{-4}	9.72×10^{-4}	65	53
m-ABB	3.97×10^{-5}	1.80×10^{-4}	7	10
p-ABB	1.56×10^{-4}	6.74×10^{-4}	28	37
Sum	$\mathbf{5.56 \times 10^{-4}}$	$\mathbf{1.83 \times 10^{-3}}$		
o-c-BPB	7.63×10^{-5}	4.25×10^{-4}	71	78
m-c-BPB	2.25×10^{-6}	ND[a]	2	ND[a]
p-c-BPB	2.81×10^{-5}	1.21×10^{-4}	26	22
Sum	$\mathbf{1.07 \times 10^{-4}}$	$\mathbf{5.46 \times 10^{-4}}$		
o-t-BPB	4.06×10^{-4}	2.15×10^{-3}	60	62
m-t-BPB	5.70×10^{-5}	2.95×10^{-4}	8	8
p-t-BPB	2.11×10^{-4}	1.04×10^{-3}	31	30
Sum	$\mathbf{6.74 \times 10^{-4}}$	$\mathbf{3.49 \times 10^{-3}}$		

[a] Not detected (below the detection limit of the FID).

Table 6
Products formed (expressed in moles) during 6 h of reaction with allyl alcohol, and allyl acetate as alkylating agent and toluene as substrate on H-USY (Si/Al 15) at 200 °C

	Product	Formula	Product formed in 6 h TOS (mol)	
			Allyl alcohol	Allyl acetate
Side products of alkylating agent	Propene	C_3H_6	1.27×10^{-4}	9.37×10^{-5}
	Propanal	C_3H_6O	4.49×10^{-4}	9.42×10^{-6}
	Propanol	C_3H_8O	2.74×10^{-4}	–
	Ethyl acetate	$C_4H_8O_2$	–	–
	Propyl acetate	$C_5H_{10}O_2$	–	–
	Acetic acid	$C_2H_4O_2$	–	2.42×10^{-3}
	Diallyl ether	$C_6H_{10}O$	7.86×10^{-5}	
	1,2-PDDA	$C_7H_{12}O_4$	–	–
	Sum (side products of AA)		$\mathbf{9.29 \times 10^{-4}}$	$\mathbf{2.53 \times 10^{-3}}$
Intermediate fraction: desired alkylation products	Allyl toluene	$C_{10}H_{12}$	3.85×10^{-4}	7.37×10^{-4}
	Sum (intermediate fraction)		$\mathbf{3.85 \times 10^{-4}}$	$\mathbf{7.37 \times 10^{-4}}$
Heavy fraction	**Sum (heavy fraction)**		$\mathbf{1.07 \times 10^{-3}}$	$\mathbf{1.32 \times 10^{-3}}$
Total turn over number (molecules/acid site)			**62.1**	**70.1**
Alkylation turn over number (molecules/acid site)			**1.8**	**3.5**

activity in allyl acetate conversion and slower deactivation (Fig. 6a). Moreover, allyl toluene is nearly not present in the beginning of the run, appearing only when the catalyst starts to deactivate (Fig. 6). However, it appears that most of the formed alkylation products in the toluene reaction are transformed further into heavier components, containing two, three, or even four aromatic rings, which were not formed with bromobenzene. The total amount of heavy components is about one order of magnitude higher with toluene (Tables 4 and 6). Secondary reactions occur more easily with toluene than with bromobenzene because of the activated character of toluene.

In the reactions with allyl alcohol, a completely different product distribution is obtained for both substrates (Figs. 4c and 6b; Tables 4 and 6). With toluene, the major component group consists of a heavy fraction containing poly-aromatic components, with a small amount of primary alkylation products. In the beginning of the run, the reaction selectivity toward this group of polyaromatics was 100%, but increasing TOS brought an increased relative contribution of allyl toluene, diallyl ether, and a light fraction (consisting of propene, propanal, and propanol) to the product stream (Fig. 7). The higher intrinsic reactivity of toluene compared with bromobenzene resulted in secondary reactions between allyl toluene and toluene, similar to what was observed in the alkylation of toluene with allyl acetate. Because of the decreased catalyst activity with time and the gradual filling of the zeolite pores with coke or polymers, these secondary reactions are moderated, and primary alkylation products elute from the catalyst bed.

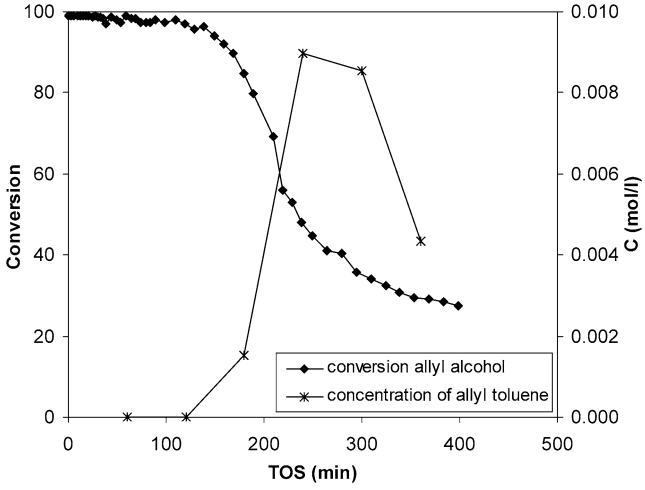

Fig. 7. Increase in allyl toluene concentration with decrease in catalytic activity in the alkylation of toluene with allyl alcohol on H-USY (Si/Al 15) (200 °C, LHSV = 57.6 h^{-1}).

4. Conclusions

In the present work we have demonstrated that acidic zeolites allow functionalization of strongly deactivated halogenated aromatic substrates using bifunctional alkylating agents. But important deactivation, competitive adsorption effects, and unwanted side reactions complicate this difficult alkylation reaction. In the alkylation of bromobenzene with allyl chloride or 1-octen-3-ol, the product stream consisted mainly of unwanted side products resulting from side reactions of the alkylating agent, and secondary alkylation reactions leading to formation of heavy components. With allyl alcohol and allyl acetate, significant formation of primary alkylation products (i.e., allyl bromobenzene, *cis*-2-propenyl bromobenzene, and *trans*-2-propenyl bromobenzene) was observed. Because of its very selective adsorption, allyl alcohol is enriched in the zeolite pores, leading to side reactions and formation of breakdown components of allyl alcohol. Allyl acetate is less selectively adsorbed, leading to a more homogeneous distribution of the substrates bro-

mobenzene and allyl acetate in the zeolite pores compared with allyl alcohol, and consequently more efficient alkylation of bromobenzene. When toluene was used as substrate, much more heavy products and less primary alkylation products were formed as a result of the higher intrinsic reactivity of toluene compared with bromobenzene. In this case the primary alkylation products were further transformed into heavier components in secondary reactions between allyl toluene and toluene. Milder reaction conditions could reduce these secondary reactions with toluene. In all of the tested reactions, strongly adsorbing components were formed that gradually fill up the micropores and cause deactivation in the catalyst. In the next part of this study, we investigate the alkylation of bromobenzene with allyl acetate in more detail, considering the influence of zeolite and feed composition, contact time, and temperature.

Acknowledgments

This research was supported by FWO Vlaanderen (G.0231.03N). J. Denayer received a FWO-Vlaanderen fellowship as a postdoctoral researcher. The CHIS and COK teams participate in the IAP-PAI Program on Supramolecular Chemistry and Catalysis sponsored by the Belgian government.

References

[1] K. Tanabe, W.F. Hölderich, Appl. Catal. A 181 (1999) 399.
[2] G.A. Olah, V.P. Reddy, G.K.S. Prakash, Kirk–Othmer Encyclopedia of Chemical Technology, vol. 11, fourth ed., Wiley–Interscience, New York, p. 1042.
[3] M. Zaidlewicz, J. Cytarska, A. Dzielendziak, M. Ziegler-Borowska, Arkivoc (III) 11 (2004), issue in honor of Prof. Markosza.
[4] W.F. Hölderich, H. van Bekkum, in: H. Van Bekkum, E.M. Flanigen, P.A. Jacobs, J.C. Jansen (Eds.), Introduction to Zeolite Science and Practice, second completely revised and expanded ed., Stud. Surf. Sci. & Catal., vol. 137, Elsevier, Amsterdam, 2001, p. 821.
[5] J.S. Beck, W.O. Haag, in: G. Ertl, H. Knözinger, J. Weitkamp (Eds.), Handbook of Heterogeneous Catalysis, vol. 5, Wiley–VCH, Weinheim, 1997, p. 2123.
[6] P. Espeel, R. Parton, H. Toufar, J. Martens, W. Hölderich, P.A. Jacobs, in: J. Weitkamp, L. Puppe (Eds.), Catalysis and Zeolites, Fundamentals and Applications, Springer Verlag, Heidelberg, 1999, p. 377.
[7] H.W. Kouwenhoven, H. van Bekkum, in: G. Ertl, H. Knözinger, J. Weitkamp (Eds.), Handbook of Heterogeneous Catalysis, vol. 5, Wiley–VCH, Weinheim, 1997, p. 2358.
[8] P. Metivier, in: R.A. Sheldon, H. van Bekkum (Eds.), Fine Chemicals through Heterogeneous Catalysis, Wiley–VCH, Weinheim, 2001, p. 161.
[9] C. Perego, P. Ingallina, Catal. Today 73 (2002) 3–22.
[10] E.G. Derouane, C.J. Dillon, D. Bethell, S.B. Derouane-Abd Hamid, J. Catal. 187 (1999) 209.
[11] E.G. Derouane, G. Crehan, C.J. Dillon, D. Bethell, H. He, S.B. Derouane, J. Catal. 194 (2000) 410.
[12] A.E.W. Beers, T.A.X. Nijhuis, F. Kapteijn, J.A. Moulijn, Microporous Mesoporous Mater. 48 (2001) 279.
[13] A.E.W. Beers, T.A.X. Nijhuis, N. Aalders, F. Kapteijn, J.A. Moulijn, Appl. Catal. A 243 (2003) 237.
[14] A.E.W. Beers, J.A. van Bokhoven, K.M. de Lathouder, F. Kapteijn, J.A. Moulijn, J. Catal. 218 (2003) 239.
[15] C. Castro, A. Corma, J. Primo, J. Mol. Catal. A 177 (2002) 273.
[16] F.J. Llopis, G. Sastre, A. Corma, J. Catal. 227 (2004) 227.
[17] I.I. Ivanova, V. Montouillout, C. Fernandez, O. Marie, J.P. Gilson, Microporous Mesoporous Mater. 57 (2003) 297.
[18] X.C. Hu, G.K. Chuah, S. Jaenicke, Microporous Mesoporous Mater. 53 (2003) 153.
[19] G. Langhendries, D.E. De Vos, G.V. Baron, P.A. Jacobs, J. Catal. 187 (1999) 453.
[20] G. Langhendries, G.V. Baron, P.E. Neys, P.A. Jacobs, Chem. Eng. Sci. 54 (1999) 3563.
[21] M.J. Remy, D. Stanica, G. Poncelet, E.J.P. Feijen, P.J. Grobet, J.A. Martens, P.A. Jacobs, J. Phys. Chem. 100 (1996) 12440.
[22] F. Collignon, M. Mariani, S. Moreno, M. Remy, G. Poncelet, J. Catal. 166 (1997) 53.
[23] I. Daems, P. Leflaive, A. Méthivier, J.F.M. Denayer, G.V. Baron, Microporous Mesoporous Mater. 82 (2005) 191.
[24] U. Lohse, B. Parlitz, J. Phys. Chem. 93 (1989) 3677.
[25] C. Peirera, G.T. Kokotailo, R.J. Gorte, J. Phys. Chem. 94 (1990) 2063.
[26] A. Boréave, A. Auroux, C. Guimon, Microporous Mater. 11 (1997) 275.